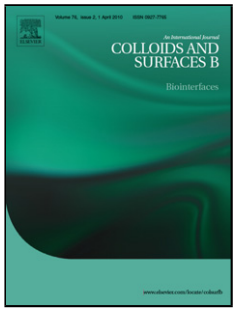

Title: Drug release mechanisms of chemically cross-linked albumin microparticles: Effect of the matrix erosion

Author: Danielly L.A. Sitta Marcos R. Guilherme Elisangela P. da Silva Artur J.M. Valente Edvani C. Muniz Adley F. Rubira

PII: S0927-7765(14)00376-2
DOI: http://dx.doi.org/doi:10.1016/j.colsurfb.2014.07.014
Reference: COLSUB 6529

To appear in: *Colloids and Surfaces B: Biointerfaces*

Received date: 17-2-2014
Revised date: 8-7-2014
Accepted date: 11-7-2014

Please cite this article as: D.L.A. Sitta, M.R. Guilherme, E.P.S. </sup>Artur J.M. Valente, E.C. Muniz, A.F. Rubira, Drug release mechanisms of chemically cross-linked albumin microparticles: effect of the matrix erosion, *Colloids and Surfaces B: Biointerfaces* (2014), http://dx.doi.org/10.1016/j.colsurfb.2014.07.014

GRAPHICAL ABSTRACT

Drug release mechanisms of chemically cross-linked albumin microparticles: effect of the matrix erosion

Danielly L. A. Sitta, Marcos R. Guilherme, Elisangela P. da Silva, Artur J. M. Valente, Edvani C. Muniz, and Adley F. Rubira

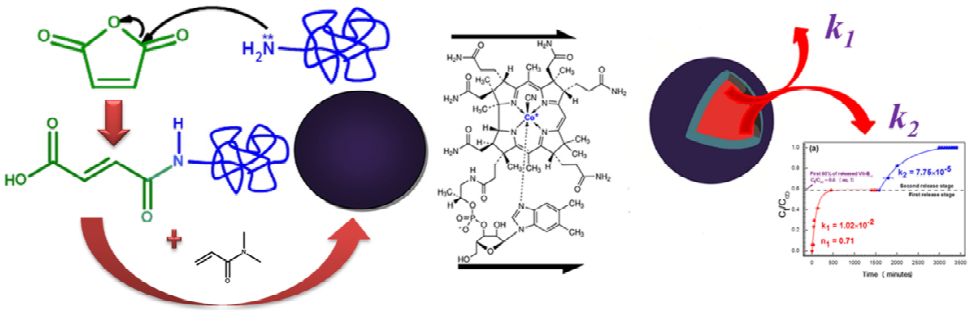

251658240

Research Highlights

- Albumin (BSA) microparticles were obtained in a W/O emulsion without and with PVA
- BSA played a role as a surface active agent for W/O emulsion, replacing PVA
- The microparticles showed a two-stage drug release profile at pH 2, 6 and 10
- The two-step release mechanism is a characteristic of the BSA microparticles
- The second release stage is a contribution of the matrix erosion

Drug release mechanisms of chemically cross-linked albumin microparticles: effect of the matrix erosion

Danielly L. A. Sitta,[a] Marcos R. Guilherme,[a] Elisangela P. da Silva[a] Artur J. M. Valente,[b] Edvani C. Muniz,[a] and Adley F. Rubira[a*]

[a]*Department of Chemistry, State University of Maringá, Av. Colombo, 5790, CEP 87020-900, Maringá, Paraná, Brazil*

[b]*Department of Chemistry, University of Coimbra, 3004 535 Coimbra, Portugal*

List of the total number of words and tables/figures

(i) Words 5984

(ii) Tables 2

(iii) Figures 6

Abstract

Albumin (BSA) microparticles were developed as a biotechnological alternative for drug delivery. Vitamin B_{12} (Vit-B_{12}) was used as a model drug. The microparticles were obtained from maleic anhydride-functionalized BSA and *N',N'*-dimethylacrylamide (DMAAm) in a W/O emulsion without and with PVA. The microparticles produced at 15 min of stirring without PVA showed the best results in terms of size, homogeneity, and

*Corresponding author: afrubira@uem.br phone: ++ 55 44 3011 3687 FAX ++ 55 44 3261-4125

sphericity. In such a case, BSA played a role as a surface active agent, replacing PVA. For longer stirring times, BSA was unable to act as an emulsifier.

These microparticles showed an uncommon release profile, consisting of a two-step release mechanism, at the pH range studied. Considering that a two-step release mechanism is occurring, the experimental data were adjusted by applying modified power law and Weibull equations in order to describe release mechanism *n* and release rate constant *k*, respectively. Each one of the release stages was related to a specific value of *n* and *k*. The second stage was driven by a super case II transport mechanism, as a result of diffusion, macromolecular relaxation, and erosion. A third model, described by Hixson-Crowell, confirmed the erosion mechanism.

Vit-B_{12} diffusion kinetics in aqueous solutions (i.e., without the microparticles) follows a one-step process, being *k* dependent on the pH, confirming that the two-step release mechanism is a characteristic profile of the developed microparticles. The microparticles released only 2.70% of their initial drug load at pH 2, and 58.53%
at pH 10.

Keywords: Albumin; drug delivery; emulsion; erosion; microparticles; drug release kinetics

Introduction

One of the most promising areas of particles is the research and development of new pharmaceutical formulations, being that the main application is aimed towards the drug delivery. Among the various materials used in the production of nano and microparticles, there has been a considerable interest in the proteins as a starting substance for synthesis of more sophisticated release systems that may preserve the molecular structure of more potent and specific drugs [1]. This is because the protein-based materials are biodegradable, nonantigenic, and susceptible to metabolization, and also are able to be chemically modified by surface reaction for further covalent fixation of drugs and/or ligands [2].

Serum albumins are the most studied and applied proteins owing to their wide availability, low cost, good structural stability, binding properties with unusual ligands, biodegradability, and non-antigenicity [3, 4-6]. There is a great deal of interest both from a large segment of the pharmaceutical industry and from researchers in the area of biotechnology in the application of albumin as a drug carrier [7]. A remarkable property of albumin is its ability to reversibly bond to a wide variety of molecules [8], which is an interesting characteristic for drug delivery systems. Both bovine serum albumin (BSA) and human serum albumin (HSA) are used in the production of nano/microparticles [1-3, 9-12] in view of their structural similarity that corresponds to 75% of the homologous sequence. BSA is more suitable for *in vivo* tests due to its lower cost.

To synthetize BSA particles, a radical cross-linking/polymerization approach in a hydroalcoholic emulsion was used, owing its advantages for ease and quick preparation [13]. The stability of an emulsion is related both to chemical nature of interfacial film and to attraction/repulsion force balance occurring among the particles suspended in the liquid, which are important in the prevention of the coalescence [14].

Surfactants (also called emulsifying agents) adsorb on interface reducing the interfacial tension. Many amphiphilic substances that form films are stabilizers for emulsions. Some exemples are proteins (BSA, casein), glucosides, lipids, steroids, calcium carbonate, glycerol, mercuric iodide [14], and polymers such as poly(vinyl alcohol) (PVA). The advantages of the polymerization in the emulsion include: (i) quick polymerization, (ii) products with a high molecular weight [13], and (iii) well-defined stages and simple

preparation. Thus, the polymerization in emulsion is an attractive approach to produce microparticles from hydrophilic natural materials [15].

This work aimed at producing protein microparticles from BSA using a hydroalcoholic emulsion for use in drug delivery systems. Vitamin B_{12} (Vit-B_{12}) was used as the model drug. To obtain such a system, BSA was modified with maleic anhydride (MAy) in water, because only a small number of proteins may sustain dissolution in an organic medium without their molecular recognition properties being lost [16]. The nucleophilic groups in BSA, which could react with MA, are thiols of cysteine, hydroxyls of serine and tyrosine, and amines in the side chains of lysine [17]. However, the thiol groups (seventeen of them) are involved in disulfide bridges that aid to support the tertiary structure of the protein, except cys-34, because its hydroxyls are less nucleophilic and do not react under mild experimental conditions. In the present work, the reaction was processed at temperature of 37 ºC and at pH 5.5. In such a case, only a small number of accessible sterically amine groups in the side chains of lysine react under such conditions [17]. In the light of this assessment, it could be said that MAy bonds to amine groups of lysine in BSA by nucleophilic reaction introducing its functional groups to the protein structure. The bindings between the functionalized BSA and DMAAm are of covalent nature. The advantage of covalent bindings is that they are stable with time. The idea was to use the vinyl bonds in functionalized BSA (BSA^{MAy}) as a radical cross-linking/polymerization approach for reaction with *N',N'*-dimethylacrylamide (DMAAm) in the emulsion. Figure 1 shows a schema of the chemical reactions for the cross-linking of BSA. Inside particle, DMAAm serves as a network support, owing to its good gelling capacity, and do not affect the original properties of the protein such as biocompatibility and biodegradability. Furthermore, DMAAm is a safe material for use in drug delivery systems and is more indicated for such applications than acrylamide that has a great potential to cause cancer. Furthermore, DMAAm has been widely used in the preparation of biomaterials [18-20].

Insert Figure 1

Materials and Methods

Materials

Bovine serum albumin, BSA ($M_w \cong 68{,}000$ g mol^{-1}, ≥98.0%), maleic anhydride, MAy (≥99.0%), ammonium persulfate, APS, (≥98.0%) and vitamin B_{12} (≥98.5%) were purchased from Sigma-Aldrich. *N',N'*-dimethylacrylamide, DMAAm (≥99 %) and poly(vinyl alcohol) - PVA (87-89% hydrolyzed, $M_w \cong 31.000$ g mol^{-1}) were obtained from Aldrich. Benzyl alcohol (99.0%) and absolute ethyl alcohol (≥99.3%) were supplied by Fmaia, whilst *N,N,N',N'*-tetramethylethylenediamine, TEMED (d = 0.780 g.mL^{-1}, ≥99.0%) was obtained from Invitrogen. For buffer solutions, sodium phosphate, dibasic, anhydrous (98.0%) were supplied by Nuclear, and potassium phosphate, monobasic, (99.0%) from Labsynth. Buffer solutions of pH 7 and 10 were obtained from Synth. The hydrochloric acid (36.5-38.0%) and sodium chloride (Synth, 99.0%) were supplied by Chemco and Synth, respectively. All chemical were used as received.

Functionalization of BSA with MAy (BSA^{MAy})

Protein-functionalizing solution was prepared by adding 0.5 g of BSA and 0.05 g of MAy to a phosphate buffer solution (0.1 M) with pH 5.5 while stirring. After homogenization, the solution was stirred for 3 h at 37 ºC. The obtained product was precipitated with cold ethanol (2 °C), subsequently separated by centrifugation at 9500 rpm, and washed with deionized-distilled water three times.

Preparation of protein microparticles using BSA^{MAy} and DMAAm

After lyophilization, 0.1 g of BSA^{MAy} was added to 5 mL of phosphate buffer solutions at pH 7.0 at 20°C while stirring. The buffer solutions were previously prepared, but using different amounts of PVA (stabilizing agent) such as 0%, 1% and 2% (w/v). Then, 52 µL of DMAAm were incorporated under inert atmosphere of argon. After the mixture turned to a transparent, clear solution, 20 mL of benzyl alcohol were added dropwise while stirring so that a whitish emulsion was immediately formed. After 30 min, 0.02 g of ammonium persulfate, as an initiating agent, and 12.5 µL of TEMED, as a catalytic agent, were added to emulsion that was stirred at 750 rpm with the use of a propeller-shaped stirrer with 60 mm of diameter. The thus obtained product was precipitated with cold ethanol (2 °C), separated by centrifugation at 9500 rpm, and washed with deionized-distilled water three times. Other microparticles were produced in the same way but using stirring times of 15, 30, 60, and 90 min.

Loading of Vit-B_{12} onto the microparticles

Two efficient approaches may be used to load a given solute onto a polymer device: (i) *post*-loading approach (after the device processing), and (ii) *in situ* loading approach (during the device processing). The *post*-synthesis loading approach is performed by immersing the microparticles into a solution containing the drug of interest. In such a case, the drug diffusion into the microparticle occurs by absorption and/or adsorption. The efficiency of such a strategy is related to affinity of the drug for protein chains. Here, the *in situ* loading approach was used in view that a more significant amount of the drug can be loaded. In the *in situ* loading one, the drug molecules are trapped into the BSA network over the cross-linking/polymerization of the protein chains. There is no binding between Vit-B_{12} and DMAAm. The carbon-carbon double bonds of Vit-B_{12} are connected to either a carbonyl group or chemical groups, which are stabilized by resonances with steric hindrance. The initial weight of Vit-B_{12} corresponded to 10% of the total weight of BSA^{MAy} used in the microsphere-forming emulsion.

Vit-B_{12} release from the microparticles

For tests of release, 0.1 g of Vit-B_{12}-loaded microparticles was added to 30 mL of buffer solutions at pH 2, pH 6 or pH 10 at 37 °C, and subsequently introduced into a dialysis tube. The suspension-filled dialysis tube was fixed at the bottom of a glass reactor with 220 mL of the corresponding buffer solution at 37 °C. The external solution was stirred at 300 rpm using a magnetic stirrer. Then, aliquots of 5 mL were collected from the external solution at specified periods, and then absorption readings were made at 360 nm in a UV-Vis spectrophotometer (Biochron, Libra S12 model). After, the aliquots were brought back into the reactor to prevent variation of volume.

Both the loading efficiency and the concentrations of Vit-B_{12} released from the microparticles were determined from an analytical curve correlating the absorption to the concentration of the drug in water. The molar extinction coefficient (ε) specific to 360 nm wavelength was 2.3×10^4 $M^{-1}cm^{-1}$.

In vitro release mechanism and release kinetics

To determine the release profile of Vit-B_{12}, curves correlating the fraction of the released drug to time were elaborated. The time-dependent release curves were calculated by the ratio between the concentration of drug released at specific time and the concentration of drug released at equilibrium. The experimental data were adjusted by applying a modified simple power law Korsemeyer-Peppas (equation 1) (see Section for further details), which is the most simple and comprehensive model used to describe the release profile of drug from a polymer device [21-24].

$$\frac{C_t}{C_\infty} = c_0 + k\left(t - [\![t_0]\!]\right)^n \quad (1)$$

where C_t and C_∞ are the cumulative concentrations of solute released from the microspheres at a specified time and at equilibrium, respectively, k is a proportionality constant that describes geometric and structural characteristics, C_0 represents the concentration of the released specie at the time-lag t_0, and n is the diffusional coefficient used to interpret the release mechanism [21-24].

The equation 1 is applied to predict the release mechanism of devices with different geometric shapes, such as films, cylinders, discs and spheres, but it is restricted for the first 60% of released solute ($C_t/C_\infty < 0.60$) [21, 22].

The values of n depend on geometry of the device. The conceptual meanings of n for geometrical shapes of the device are summarized in Table 1. Fickian diffusion indicates that the release mechanism is controlled by diffusion, that is, the drug diffuses through layers of the device. Anomalous transport is the contribution of both Fickian diffusional and relaxational mechanisms. In case II transport, the mechanism is driven by macromolecular relaxation of the polymer chains, and is independent on time. Super case II transport mechanism results of the contribution of diffusion, macromolecular relaxation, and erosion of the polymer device [22, 24, 25].

Insert Table 1

To describe the overall profile of the *in vitro* released drug, and in order to take into account that in several occasions a two-step mechanism is occurring, a slightly modified version of the Weibull function [26] has been used:

$$\frac{C_t}{C_\infty} = C_0 + \left(1 - e^{\left(-[\![k'(t-t_0)]\!]^d\right)}\right) \quad (2)$$

here, *d* and *k'* are related to mechanism and release rate constant, respectively [27]. The equation 2 gives an insight into the diffusional mechanism, since *k'* is closely related to the rate constant of release [28].

Physical-chemical characterizations

Fourier transform infrared spectroscopy (FTIR)

FTIR spectra of BSA, BSA^{MAy} and microparticles were recorded in a Bomem FT-IR model MB100 spectrometer. All the samples were introduced as dry powders. Powdered samples were prepared into pellets with KBr. The spectra were acquired in triplicate and a total of 128 scans were run for each spectrum to reach the resolution of 4 cm^{-1}.

^{1}H Nuclear Magnetic Resonance (NMR) spectroscopy for BSA^{MAy}

^{1}H NMR spectra were recorded in a Varian spectrometer, model Mercury Plus BB 300 MHz, using a frequency of 300.059 MHz, an angle pulse of 90° and a relaxation delay of 30 s. For spectra acquisition, D_2O solutions (0.7 mL) containing either 20 mg L^{-1} of BSA or 20 mg L^{-1} of BSA^{MAy} were prepared using 3-(trimethylsilyl)propionic-2,2,3,3-d_4 acid sodium salt ((TSP-d_4 (0.05%)) as internal reference. The resonance assigned to water was suppressed by irradiation during the relaxation.

Solid-state ^{13}C-CP/MAS NMR spectroscopy for microparticles

The solid-state ^{13}C-CP/MAS NMR spectra of BSA, BSA^{MAy} and microparticles were obtained using angle pulse of 37º, frequency of 75.45 MHz, contact time of 3 ms, and relaxation time of 3 s.

Measures of dynamic light scattering (DLS) and ζ- potential

Diluted suspensions of microspheres were prepared with addition of a very small quantity of sample to 1.5 mL of water at room temperature while stirring. After 15 min of dispersion, the suspension became clear because of dilution. Later, 1.5 mL of the stirred suspension were introduced into a glass cell for DLS analysis. The diameters of water-dispersed particles were determined from intensity size distributions using a Nano Particle Size and Zeta Potential DLS analyzer from Particulate Systems. Data were processed with the use of a software supplied by own manufacturer. The readings of *ζ*- potential were made with the injection of 0.7 mL into a standard sample flow cell under the desired temperature. The values were recorded at room temperature using stirred suspensions of microparticles.

Scanning electron microscopy (SEM) for morphology

Morphological characteristics of the lyophilized samples were analyzed in a scanning electron microscope (Shimadzu, model SS 550 Superscan). The samples were earlier sputter-coated with a thin layer of gold. SEM images were made applying an acceleration voltage of 15 kV and a current intensity of 30 μA.

Results and discussion

Spectroscopic characterization of functionalized BSA and microparticles

Figure 2(a) shows the FTIR spectra of BSA, BSA^{MAy}, and microparticles prepared at stirring times of 15, 30, 60 and 120 min. The band at 947 cm^{-1} in the FTIR spectrum of BSA^{MAy}, attributed to bending vibration of disubstituted C=C groups, indicates the functionalization of the protein. This band disappeared completely in the spectra of the microparticles after the cross-linking/polymerization reaction, because of the consumption of carbon-carbon π-bond. Furthermore, this vibrational mode also suggests a *trans* conformation [29], indicating a change from *cis* (original conformation) to *trans* owing to maleic anhydride ring-opening over the modification reaction. If the isomeric conformation of the double bond of MA supposedly was cis, a band of high intensity should appear in the region of 730-665 cm^{-1}, owing to =C-H bending [29]. The presence of $H_2PO_4^-/HPO_4^{2-}$ mineral acid in the phosphate buffer solution of pH 5.5, used in the reaction, could have influenced on the spatial conversion of the double bond, and this seems to be the case of BSA^{MAy}.

Figure 2(b) shows the ^1H NMR of BSA and BSA^{MAy}. The signals at δ 5.8 and δ 6.2 in the spectrum of BSA^{MAy} were assigned to vinyl carbon-bonded hydrogen resonances in the functionalized protein, which confirms the formation of BSA^{MAy}, supporting the FTIR analysis. This approach was complemented by solid-state ^{13}C-CP/MAS NMR spectroscopy (Figure 2(c)). The signals at δ 127 and δ 132 were attributed to carbonyl carbon of acids in conjugated systems, which are absent in the original structure of BSA. The introduction of chemical groups from MAy to BSA creates vinyl acids (-HC=CH-COOH) in the protein.

From the analysis of Figure 2(c) it can also be observed in the spectrum of BSA^{MAy} a reduction of the resonance intensity at δ 29 ppm, and the appearance of a new resonance at δ 36. These spectral changes indicate that the amine groups in BSA reacted to form primary, secondary and tertiary amines in BSA^{MAy}. The occurrence of the cross-linking polymerization reaction of BSA^{MAy} with DMAAm was verified by the reduction in the intensity of the signal at δ 167 in the spectrum of microparticles, corroborating the FTIR data. Although the region of the vinyl groups (δ 127 and δ 132), in the spectrum of BSA^{MAy}, was somewhat overlapped by signal of benzyl alcohol residues, in the spectrum of particles, significant changes may be observed in the same spectral region. This represents an additional evidence of the particle formation.

Insert Figure 2

Microparticle Morphology

The objective of using a W/O emulsion as a cross-linking/polymerization approach was based on the concept that this reaction medium is effective to produce polymer microparticles with an approximately spherical shape. Well-defined microparticles show regular mass distribution, which may prevent both anisotropic swelling and deviation of ideal release profile [11,30]. Furthermore, the size and shape of these microparticles could be improved with aid of partially hydrolyzed PVA [31].

In the emulsion cross-linking/polymerization, speed and time of stirring, and amount of surfactant affect the morphology of the microparticle. Here, the stirring speed used for protein-based microparticles was relatively low (750 rpm), compared with those of the literature: 6100 rpm [32], 1500 rpm [33], and 1000 rpm [1, 11, 30]. From a physical chemical point of view, our present understanding is that the structural

integrity of BSA may be affected at a stirring speed higher than those that have been reported. However, stirring speeds lower than 750 rpm may not be enough to finely emulsify a W/O mixture.

Figure 3 shows the SEM images of BSA, BSA^{MAy}, and microparticles produced at different stirring times with and without PVA. The following conclusions can be taken from the SEM images: (i) BSA particles showed predominantly spherical shape with small size dispersity (Figure 3(c)), (ii) by increasing the stirring time from 15 to 30 min, the surface of the particles became rough, with heterogeneous particle dimensions (Figure 3(f)); (iii) a further increase of stirring time lead to particles with undefined shape (Figures 3(i) and 3(l)); (iv) those particles containing PVA showed an undefined shape (Figures 3(d-e)); (iv) by increasing the stirring time to 30 minutes, blend particles showed undefined shape and aggregation (Figures 3(g-h)); and (vi) increasing the stirring time for 60 and 120 minutes blend particles showed unshaped and heterogeneous size (Figures 3(j-k)) and heterogeneous size (Figures 3(m-n)), respectively.

The microparticles formed at 15 min without PVA showed the best results in terms of size, homogeneity, and sphericity. An important factor is that the proteins show emulsifying properties by adsorption on the water-oil interface, which forms a physical chemical barrier among the droplets and thus prevents the coalescence of the emulsion [34]. In such a case, BSA acted as a surface active agent. During the adsorption, the protein changes its structural conformation so that physical chemical interactions at the interface become more favorable [35,36].

The extent and speed at which the protein chains are rearranged at the interface are affected by several factors such as chain flexibility, distribution of hydrophilic/hydrophobic domains, and hydrophobicity of the oil phase. In general, the proteins lose its tertiary structure owing to adsorption at the interface, although significant amounts of non-native secondary structures are preserved [35, 37].

The emulsifying properties of BSA were preserved up to 30 min of stirring. Upon addition of PVA, there is an excess of emulsifier that affects the stability of the emulsion. Under this condition, the intermolecular attraction forces of the liquid increase, and the reaction medium coalesces. The efficiency of the protein in stabilizing emulsions depends on a variety of factors, such as concentration, pH, ionic strength, thermal treatment, stirring, and so forth [30]. We theorize that, with an increase in the stirring time from 60 to 120 min, BSA became unable to act as an emulsifier owing to an excessive denaturation that could lead to precipitation, and thus PVA starts playing such a role. Therefore, PVA improves both sphericity and homogeneity of the microparticles synthetized at longer stirring times. With the addition of PVA, there can be a competitive adsorption between the protein and the surfactant molecules at the interface, leading the emulsion to a destabilization [38,39].

The proteins and emulsifiers stabilize emulsions by different mechanisms. The proteins may be adsorbed at the interface owing to their structural characteristics. It has been reported that the proteins are able to form a hydrated layer at the interface and that some of the side-chains of the hydrophobic residues can enter a small distance into oil phase. The emulsifiers function by decreasing the interface tension and depends on the intramolecular repulsion forces among the polar groups [38,40].

Insert Figure 3

ζ- potential and dynamic light scattering (DLS)

On the basis of the SEM results, only microparticles produced at 15 min of stirring without PVA were further analyzed by DLS and ζ- potential (Figure 4). Figure 4(a) shows the ζ-potential curves of BSA, BSA^{MAy}, and microparticles produced at 15 min without PVA. The ζ-potentials were measured in water at pH of nearly 7 for all samples. Under this condition, BSA showed negative ζ- potential (−10.49 ± 0.11), because, at pH above the isoelectric point, the acid groups of the amino acid residues in the protein undergo deprotonation. The ζ- potential became more negative in BSA^{MAy} (−33.77 ± 3.32), owing to reaction between free amine and maleic anhydride that introduced new carboxylic groups to the protein. In the microparticles, the ζ- potential changed to −17.05 ± 1.25. In such a case, the amine groups in DMAAm counterbalance, to some extension, the charges on the acid groups in BSA.

Figure 4(b) shows the DLS curve of microparticles produced at 15 min without PVA. These microparticles showed an average diameter of 1.35 μm. As the particle diameter was on the order of micrometers, only a run was performed for that sample to prevent sedimentation or aggregation of particles in a layer at the bottom of the suspension, which leads to a larger particle size distribution.

The micrometer-sized particles were formed by cross-linking/polymerization reaction at the droplets of alcohol-confined water in the emulsion, owing to hydrophilic nature of BSA^{MAy} and DMAAm. The spherical shape of the microparticles results of a macromolecular fine-tuning of both reactants to water droplets during the reaction.

Insert Figure 4

Vit-B_{12} release from the microparticles

The microparticles showed a loading efficiency of 78.4 ± 1.5%, considering the initial Vit-B_{12} concentration added to the emulsion. Figures 5(a), (b) and (c) shows time-dependent release curves of Vit-B_{12} from the microparticles at 37 °C at different pH values. The experimental data were fitted according to equations 1 and 2 in order to describe release mechanism *n,* and release rate constants k'_1 (first stage) and k'_2 (second stage), respectively.

Tortuous release profiles, in which two release stages were described, were observed at the pH range studied. Each one of the release stages was related to a specific value of *n* and *k*, suggesting that the overall release profile of Vit-B_{12} from the protein-based microparticles is predicted by different types of mechanisms and release rates. These two step-release mechanisms have been found for release of DNA [41] and BSA and FITC-dextran [42] from DNA-based gels. Table 2 summarizes the data of *n* and *k* and other adjusting parameters for the two stages, where subscripts 1 and 2 represent the first and second stage, respectively.

Insert Figure 5 and Table 2

Release rate constant (k) of Vit-B_{12}

At pH 2 (Figure 5(a)), the values of *k* indicated a release rate faster in the beginning of the experiment, followed by a lag phase (or equilibrium) and a release rate approximately 8×10^{-3} times slower. The release rates at pH 6 (Figure 5(b)) and at pH 10 (Figure 5(c)) differ from those in the strongly acid medium. At pH 6, there was a slow release rate in which less than 10% of the total load of Vit-B_{12} was released, followed by a release rate two orders of magnitude faster until reaching the equilibrium. At pH 10, the release rate is initially slower and less than 20% of the drug is released, followed by a release rate approximately 52 times faster. The different release profiles result of both structural changes and charges generated on the polymer network of the microparticles, owing to changes at pH of the release medium.

The total cumulative release of Vit-B_{12} increased with increasing pH of the surrounding liquid. The microparticles released only 2.70% of their initial drug load at pH 2.

The experimental data at different pH indicated that these microparticles have a great potential for uses in the systems that release drugs at the intestine, especially at the colon, where the environment is slightly alkaline.

Release mechanism (n) of the model drug (Vit-B_{12})

The values of t_∞ of Vit-B_{12} were larger at pH 2 (Figure 5(a)) and at pH 10 (Figure 5(c)). However, at pH 6 (Figure 5(b)), t_∞ was slower than in both the acid and the basic media, owing to the lower liquid charge on BSA at pH close to its isoelectric point. Under this condition, the physical chemical affinities between BSA and Vit-B_{12} are minimized, and a larger load of the drug is released at a shorter time.

The value of n (n_1 = 0.71±0.02) at pH 2 (Figure 5(a)) indicated an anomalous mechanism for Vit-B_{12} release, coupling of Fickian diffusional and relaxational mechanisms. Only a value of n can be described for such pH, because the first release stage corresponded practically to first 60% of the released drug. This is a limit value for applicability of the equation 1. At pH 6 (Figure 5(b)), at the first release stage of the (C_t/C_∞) curve *vs* time, where the release reached 3% of the total release, the drug release follows a pseudo-Fickian mechanism (n_1 = 0.22±0.01). At the second stage, which corresponded to 60% of the total release, the mechanism is governed by super case II transport (n_2 = 2.31±0.09), contributions of diffusion, macromolecular relaxation, and erosion. At pH 10, at the first stage, the anomalous mechanism was predominant (n_1= 0.62±0.02). At the second stage, the release occurred by diffusion, macromolecular relaxation, and erosion (n_2 = 5.29±0.11). These findings are according to those reported elsewhere [43,44]. It has been reported that the drug release from the hydrophilic polymer devices is result of a glassy-to-rubbery transition caused by water penetration into the device. The two most important factors which affect swellable polymer devices are water penetration (including hydration, gelatinization, and swelling) and erosion rates [43].

Influence of morphology on the release

To verify the influence of the morphology on the release, the samples were first swollen in buffer solutions of pH 2, pH 6 or pH 10 at 37 °C (same method of the release) and lyophilized before observation by SEM. In those conditions, it is assumed that the morphology of the swollen samples were preserved, that is, the actual morphology of the microparticles suspended in the liquid.

Figure 6(a) shows the SEM images of the lyophilized microparticles (15 min, 0% PVA) after swelling for 24 h at pH 2, pH 6 or pH 10 at 37 °C.

The microparticles degraded after swelling at pH range studied. The swollen particles became larger (compared with those of Fig. 3(a)) and showed a hollow center. This morphology results of a burst of vesicular structure, as a consequence of osmotic pressure during the swelling.

Further insight into the release mechanism is obtained by fitting the amount of drug remaining in the matrix at time t, Q, to the Hixson-Crowell cubic root equation [45]:

$$Q^{\frac{1}{3}} = Q_0^{\frac{1}{3}} - k_c t \qquad (3)$$

where Q_0 is the amount of drug in the matrix at t = 0 and k_C is the cube root law rate constant. This equation describes the release from systems where a change in surface area and diameter of particles occurs.

Figure 6(b) shows the cube root of Vit-B_{12} remaining in the albumin microparticles plotted against time. It is also be expectable that the Vit-B_{12} release will change, by dissolution, the surface area and gel matrix dimensions. In fact, a good fitting to the Hixson-Crowell cubic root equation (equation 3) is obtained confirming that assumption. Furthermore, the applicability of the data to Hixson-Crowell model corroborates the argument that, for each pH, there are two distinct release stages. It is also possible to conclude that, in view of the mathematical fit, the erosion occurs by erosion of two layers.

Vit-B_{12} diffusion outwards dialysis tube

To check a possible influence of the dialysis tube on the tortuous release profile, 0.01 g of Vit-B_{12} was added to 30 mL of buffer solutions with pH 2, pH 6 or pH 10 at 37 °C while stirring. The conditions of the analysis were the same of the release method, but in the absence of microparticles. The Vit-B_{12} diffusion was monitored by spectrophotometry at 360 nm, and its concentrations were determined from the analytical curve. The data were shown in Figure 6(c).

The Vit-B_{12} diffusion outwards dialysis tube exponentially increased with time and only a value of *k* can be described for each pH: 1.44×10^{-3} min^{-1} for pH 2, 1.05×10^{-3} min^{-1} for pH 6, and 9.91×10^{-4} min^{-1} for pH 10. These values were almost in the same order of magnitude for the pH range analyzed, indicating that the tortuous release profile is a characteristic of the developed microparticles. Furthermore, the exponential-like diffusion curves indicated that the Vit-B_{12} do not undergoes degradation.

Insert Figure 6

Conclusions

BSA microparticles with an average diameter of 1643 μm were produced using vinylated BSA and DMAAm in the hydroalcolic emulsion, under a stirring speed of 750 rpm, for applications in drug delivery. The microparticles (15 min of stirring, 0% PVA) showed the best results in terms of size, homogeneity, and sphericity. In such a case, BSA played a role as a surface active agent, replacing PVA. The emulsifying properties of BSA were preserved up to 30 min. For longer stirring times, BSA became unable to act as an emulsifier, and PVA started playing this role.

BSA showed negative ζ- potential (–10.49 ± 0.11), because of the deprotonation of acid groups in the amino acid residues at pH 5.5. The ζ- potential became more negative in BSA^{MAy} (–33.77 ± 3.32), owing to reaction between free amine and maleic anhydride that introduced new carboxylic groups to the protein. In the microparticles, the ζ- potential changed to –17.05 ± 1.25, as a result of the amine groups in DMAAm that counterbalanced the charges on the acid groups in BSA.

Tortuous release profiles, in which two release stages were described, were observed at the pH range studied. The different release profiles, in a same kinetic curve, result of both structural changes and charges

generated on the polymer network of the microparticles owing to changes at pH. The second stage is driven by a super case II transport mechanism, as a result of diffusion, macromolecular relaxation, and erosion. Hixson-Crowell model confirmed the erosion mechanism of the microparticles. The swollen particles became larger and showed a hollow center. This morphology results of a burst of vesicular structure, as a consequence of osmotic pressure during the swelling.

The Vit-B_{12} diffusion outwards dialysis tube, without microparticles, exponentially increased with time, indicating that the tortuous release profile is a characteristic of the microparticles. The microparticles released only 2.70% of their initial drug load at pH 2, and 58.53% at pH 10.

Acknowledgments

D.L.A.S. thanks CAPES for master degree fellowship. M.R.G. thanks the CAPES/PNPD for post-doctorate fellowship. A.F.R. acknowledges the financial supports given by CNPq, INOMAT and Fundação Araucária–Brasil. Financial support from FCT/CAPES (project N.º 329/13) is also gratefully acknowledged.

References

[1] F. Iemma, U.G. Spizzirri, R. Muzzalupo, F. Puoci, S. Trombino, N. Picci, Colloid Polym. Sci. 283 (2004) 250-256.

[2] M. Jahanshahi, Z. Babaei, Afr. J. Biotechnol. 7 (2008) 4926-4934.

[3] Y. Han, S. Li, X. Wang, X. Cao, L. Jia, J. Li, Colloid Polym. Sci. 284 (2005) 203-207.

[4] E.L. Gelamo, C.H.T.P. Silva, H. Imasato, M. Tabak, Biochim. Biophys. Acta 1594 (2002) 84-99.

[5] S.Y. Kazemi, S. M. Abedirad, The Scientific World J. 2012 (2012) 1-8.

[6] D.C. Carter, X-M. He, S.H. Munson, P.D. Twigg, K.M. Gernert, B. Broom, T.Y. Miller, Science 244 (1989) 1195-1198.

[7] B. Elsadek, F. Kratz, J. Control. Release 157 (2012) 4-28.

[8] F.A. De Wolf, G.M. Brett, Pharmacol. Rev. 52 (2000) 207-236.

[9] M.-C. Lévy, D. Hettler, M.-C. Andry, P. Int. J. Pharm. 69 (1991) R1-R4.

[10] F. Edwards-Levy, M.-C. Andry, M.-C. Lévy, Int. J. Pharm. 103 (1994) 253-257.

[11] F. Iemma, U. G. Spizzirri, F. Puoci, R. Muzzalupo, S. Trombino, R. Cassano, S. Leta, N. Picci, Int. J. Pharm. 312 (2006) 151-157.

[12] J. J. Torrado, L. Illurn, S. S. Davis, Int. J. Pharm. 51 (1989) 85-93.

[13] C. P. Reis, R. J. Neufeld, A. Ribeiro, F. Veiga, Nanomed. Nanotech. Biol. Med. 2 (2006) 8-21.

[14] A. W. Adamson, A. P. Gast, Physical Chemistry of Surfaces. sixth ed., John Wiley & Sons, Inc, New York, pp. 206, 500-516, 1997.

[15] A. Shi, D. Li, L. Wang, B. Li, B. Adhikari, Carbohydr. Polym. 83 (2011) 1604-1610.

[16] C. Ladavière, T. Delair, A. Domard, C. Pichot, B. Mandrand, J. Appl. Polym. Sci. 72 (1999) 1565-1572.

[17] F. Iemma, U.G. Spizzirri, F. Puoci, G. Cirillo, M. Curcio, O.I. Parisi, N. Picci, Colloid Polym. Sci. 287 (2009) 779-787.

[18] A.P. Chiriac, L.E. Nita, M.T. Nistor, L. Tartau, Int. J. Pharm. 456 (2013) 21-30.

[19] K. Nakamae, T. Nizuka, T. Miyata, M. Furukawa, T. Nishino, K. Kato, T. Inoue, A.S. Hoffman, Y. Kanzaki, J. Biomater. Sci. Polymer Edn. 9 (1997) 43-53.

[20] F. Xu, T.-T. Yan, Y.-L. Luo, J. Bioact. Compat. Pol. 28 (2013) 66-85.

[21] P.L. Ritger, N.A. Peppas, J. Control. Release 5 (1987) 23-36.

[22] P.L. Ritger, N.A. Peppas, J. Control. Release 5 (1987) 37-42.

[23] R.W. Korsmeyer, R. Gurny, E. Doelker, P. Buri, N. A. Peppas, Int. J. Pharm. 15 (1983) 25-35.

[24] J. Siepmann, N.A. Peppas, Adv. Drug Delivery Rev. 48 (2001) 139-157.

[25] S.K. Prajapati, R. Richhaiya, V.K. Singh, A.K. Singh, S. Kumar, R.K. Chaudhary, J. Drug Delivery Ther. 2 (2012) 16-24.

[26] P. Costa, J.M.S. Lobo, Eur. J. Pharm. Sci. 13 (2001) 123-133.

[27] D. Costa, A.J.M. Valente, M.G. Miguel, J. Queiroz, Langmuir 27 (2011) 13780-13789.

[28] V. Papadopoulou, K. Kosmidis, M. Vlachou, P. Macheras. J. Pharm. 309 (2006) 44-50.

[29] R. M. Silverstein, F. X. Webster, D. J. Kiemle, Spectrometric Identification of Organic Compounds, seventh ed., Wiley, Somerset, 2005.

[30] F. Iemma, U. G. Spizzirri, F. Puoci, G. Cirillo, M. Curcio, O. I. Parisi, N. Picci, Colloid. Polym. Sci. 287 (2009) 779-787.

[31] M. Li, O. Rouaud, D. Poncelet, Int. J. Pharm. 363 (2008) 26-39.

[32] A.B. Macadam, Z.B. Shaft, S.L. James, C. Marriott, G.P. Martin, Int. J. Pharm. 151 (1997) 47-55.

[33] N.V. Larionova, G. Ponchel, D. Duchêne, N.I. Larionova, Int. J. Pharm. 189 (1999) 171-178.

[34] J. Rangsarid, K. Fukada, J. Colloid Interface Sci. 316 (2007) 779-786.

[35] S. Damodaran, Food proteins: an overview. In: S. Damodaran, A. Paraf (Eds.). Food proteins and their applications, Marcel Dekker, New York, p. 1-24, 1997.

[36] D. J. McClements, Curr. Opin. Colloid Interface Sci. 9 (2004) 305-313.

[37] J.L. Zhai, L. Day, M.-I. Aguilar, T.J. Wooster, Curr. Opin. Colloid Interface Sci. 18 (2013) 257-271.

[38] J. P. R. Day, P. D. A. Pudney, C. D. Bain, PCCP 12 (2010) 4590e4599.

[39] E. Dickinson, Food Hydrocolloids 25 (2011) 1966-1983.

[40] E. Dickinson, Colloid Surf. B-Biointerfaces 20 (2001) 197-210.

[41] C. Morán, A. A. C. C. Pais, A. Ramalho, M. G. Miguel, B. Lindman, Langmuir 25 (2009) 10263-10270.

[42] D. Costa, A.J.M. Valente, M.G. Miguel, B. Lindman, Colloid Surf. A-Physicochem. Eng. Asp. 391 (2011) 80-87.

[43] R-H. Juang, D. Storey, J. Control. Release 89 (2003) 375-385.

[44] P. Colombo, R. Bettini, P. Santi, A. De Ascentiis, J. Control. Release 39 (1996) 231-237.

[45] A. W. Hixson, J. H. Crowell, Ind. Eng. Chem. 23 (1931) 923-931.

Figure Captions

Figure 1: Strategy for the preparation of chemically cross-linked BSA microparticles. (a) Nucleophilic reaction of amine group of lysine in BSA with MA. (b) Radical ions ($I^{\cdot}$) attacking to vinyl groups in MA-modified BSA. (c) The resultant BSA macroradical reacts with DMAAm monomers molecules by cross-linking/polymerization reaction to form covalent BSA microparticles.

Figure 2: (a) FTIR spectra of BSA, BSAMAy, and microparticles produced at different times of stirring without PVA. (b) ^{1}H NMR spectra of BSA and BSA^{MAy}. (c) Solid-state ^{13}C-CP/MAS NMR spectra of BSA, BSA^{MAy}, and microparticles (15 min, 0% PVA).

Figure 3: SEM images of BSA (a), and BSA^{MAy} (b). The microparticles produced at different stirring times with and without PVA were shown in (c) 15 min, 0% PVA; (d) 15 min, 1% PVA; (e) 15 min, 2% PVA; (f) 30min, 0% PVA; (g) 30 min, 1% PVA; (h) 30 min, 2% PVA; (i) 60 min, 0% PVA; (j) 60 min, 1%; (k) 60 min, 2% PVA; (l) 120 min, 0% PVA; (m) 120 min, 1% PVA; and (n) 120 min, 2% PVA.

Figure 4: ζ-potential (a) and DLS (b) curves of albumin microparticles (15 min, 0% PVA).

Figure 5: Time-dependent release curves of Vit-B_{12} from the albumin microparticles (15 min, 0% PVA) at 37 °C for pH 2 (a), pH 6 (b), and pH 10 (c).

Figure 6: (a) SEM images of the lyophilized albumin microparticles (15 min, 0% PVA) after swelling at 37 °C at the indicated pH for an incubation period of 24 h. (b) Hixson-Crowell cube root plots of Vit-B_{12} release from the albumin microparticles (15 min, 0% PVA) 37 °C. (c) Time-dependent diffusion curves of Vit-B_{12} outwards dialysis tube at 37 °C.

Table Captions

Table 1: Values of diffusional exponent, *n*, for polymer devices with different geometrical shapes.

Table 2: Fitting parameters of equations (1) and (2) to Vit-B_{12} release from the microparticles of BSA and DMAAm (15 min, 0% PVA) at the two stages: time necessary to cumulative release of Vit-B_{12} to reach equilibrium (t_∞), total cumulative release of Vit-B_{12} (%), diffusional coefficient (*n*) and release rate constants (k_1 and k_2).

Table 1

Diffusional exponent *n*			Release mechanism
Thin film	**Cylinder**	**Sphere**	
0.5	0.45	0.43	Fickian diffusion
$0.5 < n < 1.0$	$0.45 < n < 0.89$	$0.43 < n < 0.85$	Anomolous transport (non-Fickian)
1.0	0.89	0.85	Case II transport (zero-order release)
> 1.0	> 0.89	> 0.85	Super case II transport

Table 2

	pH		
	2	**6**	**10**
t_∞ (min)	2988 (±53, n=2)	2198 (±73, n=2)	5720 (±94, n=2)
Cumulative release (%)	2.70 (±0.12, n=2)	47.70 (±0.33, n=2)	58.53 (±0.46, n=2)
n_1	0.71 (±0.02, n=2)	0.22 (±0.01, n=2)	0.62 (±0.02, n=2)
n_2	-	2.31 (±0.09, n=2)	5.29 (±0.11, n=2)
k_1 (min^{-1})	1.02×10^{-2} ($\pm2.23\times10^{-4}$, n=2)	1.53×10^{-6}($\pm5.31\times10^{-8}$, n=2)	3.97×10^{-6} ($\pm1.12\times10^{-7}$, n=2)
k_2 (min^{-1})	7.75×10^{-5} ($\pm2.15\times10^{-6}$, n=2)	2.17×10^{-4} ($\pm0.05\times10^{-5}$, n=2)	2.06×10^{-4} ($\pm0.09\times10^{-5}$, n=2)

The fitting parameters were estimated by a least-squares approach, with a 95% level of confidence (Origin 8.0).

Figure 1

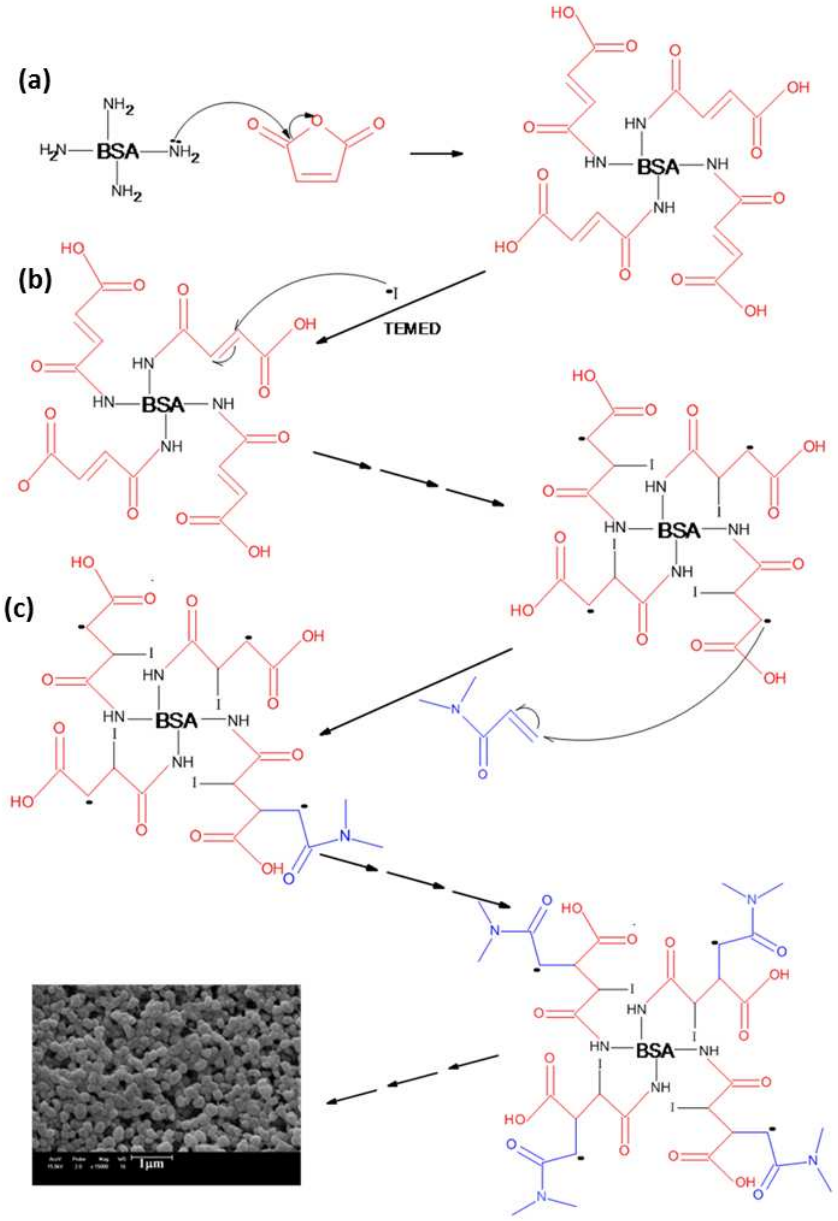

Figure 2

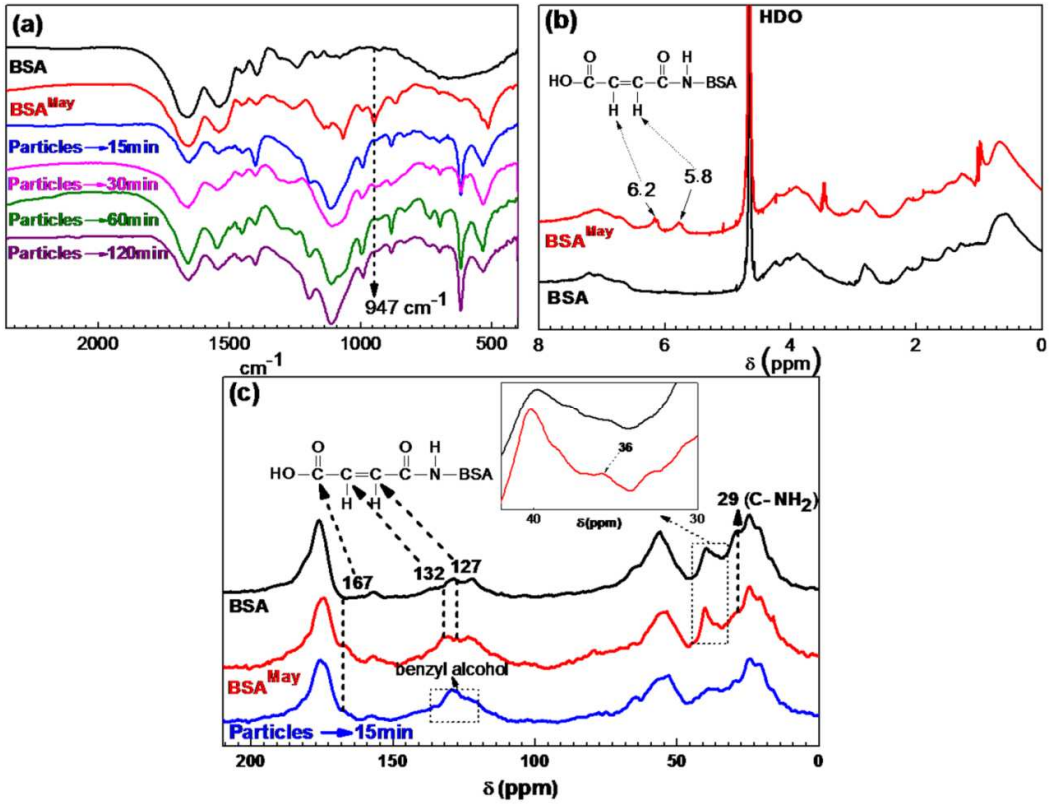

Figure 3

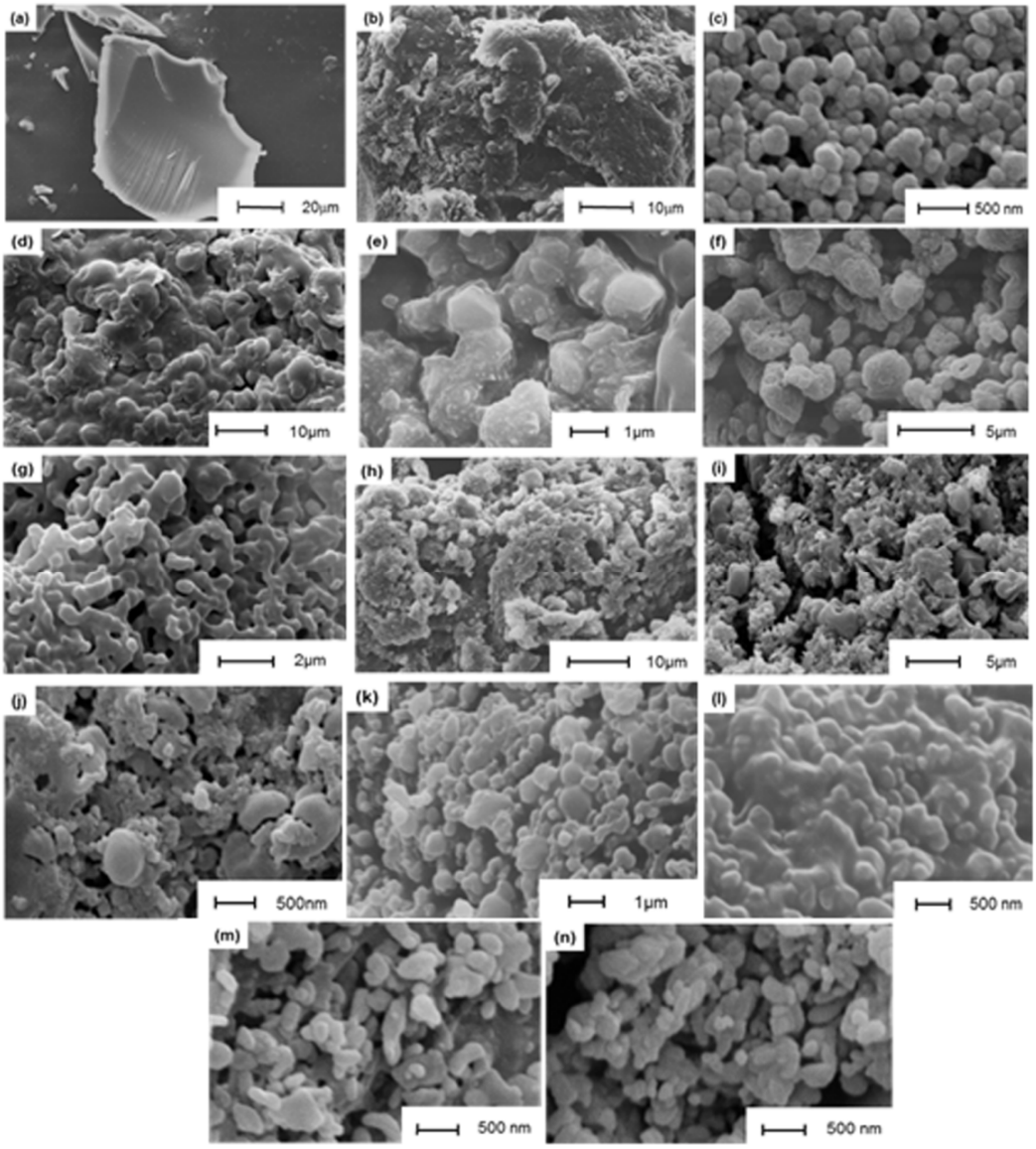

Figure 4

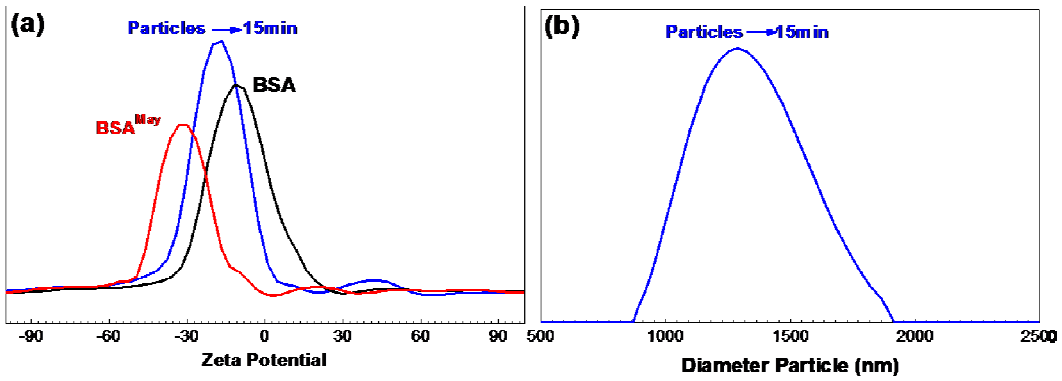

Figure 5

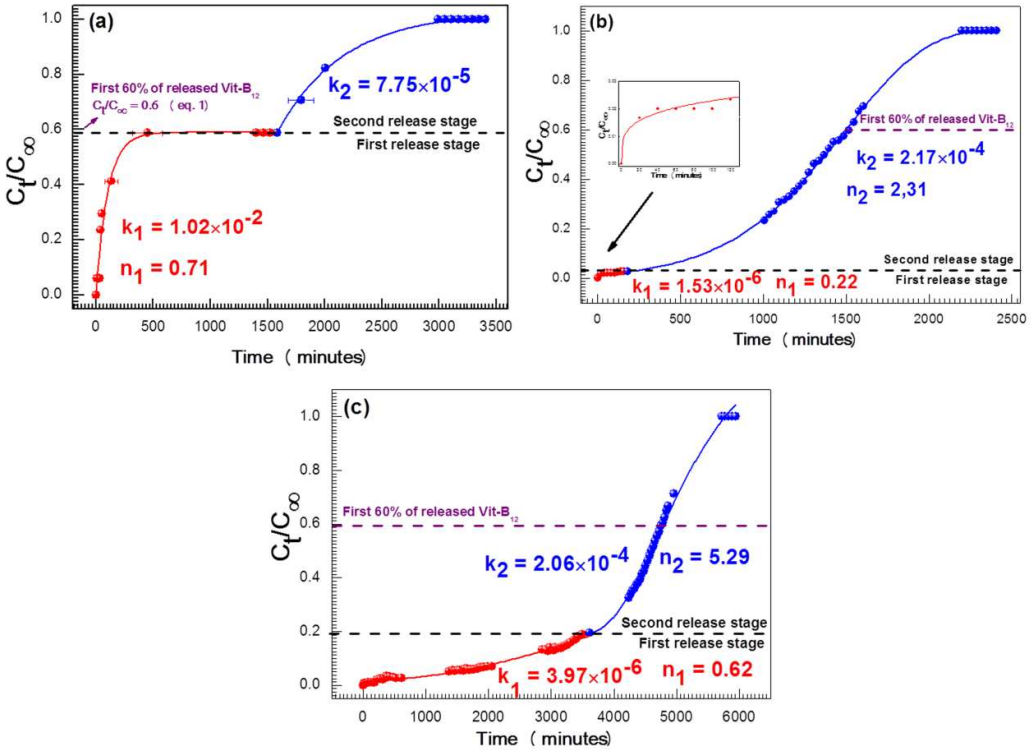

Figure 6